Patterning of platinum microelectrodes in polymeric microfluidic chips

Nazmul Huda Al Mamun
Prashanta Dutta
Washington State University
School of Mechanical and Materials Engineering
Pullman, Washington 99164-2920
E-mail: dutta@mail.wsu.edu

Abstract. Miniaturized electrodes are one of the most important components of "lab-on-a-chip" devices for separation, pumping, sensing, and other bioanalyses. In microfluidic-based chemical and bioanalytical operations, platinum electrodes are preferred to minimize the interaction with chemicals or biomolecules due to their chemical inertness. Although microfabrication techniques for patterning integrated platinum microelectrodes on silicon, quartz, or glass substrates are available, no techniques have been reported so far for depositing platinum electrodes in soft polymeric microchannels. A novel fabrication scheme is described for forming integrated microelectrodes in a poly-dimethyl-siloxane (PDMS) microchip. The electrode fabrication technique consists of photolithography, thermal processing, sequential sputtering of titanium and platinum, and stripping off photoresist, while soft lithography is used to form the microfluidic channels on PDMS. This approach facilitates precise positioning of the electrodes with a micron-size gap between them, and it can be used for both low and high aspect ratio channels. Platinum electrodes, formed on the PDMS channel surface, demonstrate very good interfacial adhesion with the substrate due to the use of a very thin titanium layer between the platinum and PDMS. The sputtered electrodes have a surface roughness of 50 nm and are able to sense picoA level current through benzene.
[DOI: 10.1117/1.2242633]

Subject terms: PDMS; Pt-electrode; microfluidic chip; strip off.

Paper 05091CR received Dec. 19, 2005; revised manuscript received Feb. 10, 2006; accepted for publication Feb. 17, 2005; published online Aug. 23, 2006.

1 Introduction

Following the trend of miniaturization, the development of microfluidic devices has been playing a significant role in recent years, especially in biological and environmental research fields. The main benefits of performing experiments in microfluidic devices are the minimal uses of sample or reagent(s), reduction in analysis time, increase in resolution in bioseparations, low thermal dispersion of sample, etc.[1,2] In the early 1990s, microfluidic devices were first fabricated in silicon wafers using micromachining techniques (photolithography and etching) adapted from the microelectronics industry. A silicon microfluidic chip not only hinders the optical detection of bioanalytical processes in it, but also is very expensive even after batch processing. In the last decade, polymeric-based materials such as poly-dimethyl-siloxane (PDMS), polymethyl-methacrylate, polycarbonate, and Teflon have received more attention as device materials.[3] Microfluidic devices made of polymeric materials can be mass-fabricated using injection molding, embossing, imprinting, laser ablation, or soft lithography.[4]

Among available polymeric materials, elastomeric PDMS is highly desirable in microfluidic applications for its characteristic of rapid prototyping with high fidelity using the soft lithography technique.[5] Some of the other advantages of using PDMS are:

1. It is optically transparent down to 280 nm, so it can be used for a number of confirmatory detection systems (UV/vis absorbance and fluorescence).
2. It can be bonded to itself or other materials both reversibly and irreversibly depending on the system requirements.
3. It is nontoxic, and it works as a perfect insulator.
4. Its surface chemistry can be controlled favorably for a number of bioanalytical operations.[2] Due to these advantages, PDMS-based microfluidic devices are used for cell, DNA, and protein separation,[2] micro-mixing,[6] electro-spray ionization mass spectrometry,[7] and fuel cells.[8]

PDMS can be bonded with a number of metals, such as titanium (Ti),[9] titanium-tungsten (TiW), gold (Au),[10] silver (Ag),[10] platinum (Pt), etc. This specific bonding characteristic enables deposition of these metals onto a PDMS surface. However, the flexibility of the PDMS layer is the major bottleneck for precise patterning of microelectrodes on a PDMS surface, especially for deep microchannels. This problem can be eliminated by bonding the PDMS channel with a glass, acrylic, or Si substrate. Gold microelectrodes can easily be patterned on a flat PDMS surface because of the availability of the gold etchant. Lee et al.[11] deposited titanium (1 nm)/gold (20 nm) electrodes on a PDMS surface by using an electron beam evaporator to demonstrate soft-contact optical lithography. However, chemically active gold reacts with sample and/or organic compounds used in bioanalytical processes and obstructs the flow inside the channel by forming bubbles. In some instances, gold electrodes disappear from the microchannel surfaces due to corrosion. Hence, chemically inert platinum is preferred as an electrode material for microfluidic-based sensing, separation, and preconcentration. There exist a number of studies where platinum electrodes were formed on different substrates, such as p-xylylene,[12] silicon

1537-1646/2006/$22.00 © 2006 SPIE

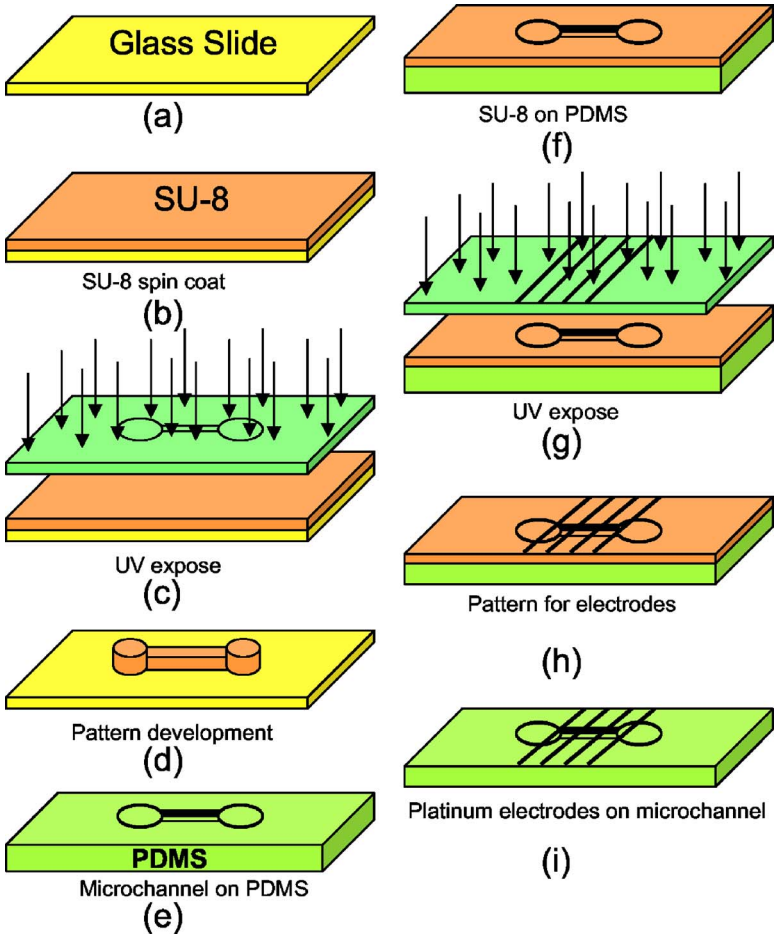

Fig. 1 Schematic view of microfabrication techniques to form the PDMS microchannel (a) to (e) and patterned electrodes around the microchannel (f) to (i).

wafer,[13] quartz,[14] and glass[15] using the lift-off process. However, no previous studies addressed the direct deposition of platinum in the flexible PDMS microchannel.

There are a number of challenges in forming platinum microelectrodes in a PDMS channel. First, it is almost impossible to etch platinum completely. A Pt-etchant (from Transene Company, Inc., Danvers Industrial Park, Danvers, Massachussets) was commercially available; however, due to inconsistent results, this product was recently discontinued. Aqua regia, a mixture of nitric and hydrochloric acids, could still be used to wet-etch platinum, but it is not advisable to use that chemical because of potential health hazards. Second, the traditional lift-off process used for patterning microelectrodes does not work for the PDMS microchannel because of the unavailability of any suitable removers for hard-baked epoxy-based photoresist.

In this communication, we describe a microfabrication technique of platinum electrodes on the PDMS microchannel surfaces using a combination of thermal processing and strip-off techniques. This method can easily be implemented in clean rooms without using hazardous chemicals. This fabrication process includes photolithography, thermal processing, sequential electrode sputtering, and stripping off the photoresist. In this study, the microchannel height was varied from 10 to 400 microns, while the designed electrode thickness was 350 nm. The length and width of the electrodes were varied from case to case.

2 Microfabrication Technique

Figure 1 shows the fabrication sequence to form the PDMS microchannel and patterned platinum microelectrodes around the channel. In this section, fabrication techniques are described for 200-μm-deep channels, and relevant parameters for 10- and 50-μm-deep channels are shown in Table 1.

PDMS microchannels were fabricated using standard photolithography and replica molding techniques. In photolithography [Figs. 1(a)–1(c)], SU-8 (MicroChem SU-8 2100) was spun (P-6000 Spin Coater, Specialty Coating Systems, Inc., Indiana) onto a glass slide (at 1550 rpm) and baked (both pre- and soft-baked) to reach the desired thickness of 200 μm. In prebaking, the photoresist-coated glass slide was heated on a hot plate (Digital Hot Plate/Stirrer, Series 04644, Cole Parmer) at 65°C for 7 min, while in soft-baking the photoresist was heated in an oven (Thelco, Model 19, Precision Scientific Company, Illinois) at 95°C for 120 min. The photoresist was then exposed to near ultraviolet light (365 nm) at 650 mJ/cm^2 using a mask

Table 1 Fabrication protocol used to form microchannels of different depths on PDMS.

	10-μm depth channel	50-μm depth channel	200-μm depth channel
Photoresist	AZ P4620	SU-8 2025	SU-8 2100
Substrate	Glass	Glass	Glass
Spin (rpm)	2000 (19 sec)	1750 (35 sec)	1550 (30 sec)
Pre-bake (°C)	N/A	65 (150 sec)	65 (7 min)
Soft-bake (°C)	80 (5 min)	95 (6 min)	95 (120 min)
Expose (mJ/cm^2)	290	380	650
Post-bake (°C)	110 (1 min)	95 (5 min)	50 (60 min)
Develop (sec)	60	150	550
Hard-bake (°C)	N/A	150 (1 min)	150 (5 min)

aligner (Hybralign, Series 500, Optical Associates, Inc., California) through direct contact with a patterned mask that contains the desired shape of the microfluidic channel. The ultraviolet radiation causes the negative resist to become polymerized, which makes it more difficult to dissolve. Next the glass slide was post-baked on a hot plate at 50 °C for 60 min. Finally, the photoresist was developed [Fig. 1(d)] with commercially available SU-8 developer (MicroChem Corp., Massachusetts). The developer solution removed only the unexposed portions of the photoresist, and the negative resist remained on the glass slide wherever it was exposed. Once the pattern was developed, two components of PDMS (pre-polymer and curing agent; Sylgard 184, Silicone Elastomer Kit, Dow Corning Corporation, Michigan) were mixed at 10:1 ratio (by volume) and degassed until no air bubbles remained in the mixture. The liquid PDMS was then poured into the mold to a height of about 5 mm. The PDMS was polymerized by curing in an oven for 3 hr at 80 °C. At the end of the curing process, the solidified PDMS layers were peeled off from the mold [Fig. 1(e)]. The resultant slab is the bottom layer of our microfluidic channel. For the top layer of the channel, an identical procedure was followed, except that two capillary tubes were attached to the mold at the appropriate locations to form inlet and exit reservoirs.

Next platinum microelectrodes were selectively formed in the PDMS channel. In this study, a highly viscous photoresist (such as SU-8 2000 series) was required to develop a pattern for electrodes in the PDMS microchannel so that the photoresist does not come out of the channel during the spin coating process. To accomplish this, PDMS surfaces with microchannel structures were spin coated (at 1000 rpm for 19 sec) with SU-8 2010 [Fig. 1(f)] and prebaked and soft-baked at 65 °C and 95 °C, respectively. This resulted in a photoresist layer about 30-μm thick. Then the photoresist was exposed [Fig. 1(g)] to near-ultraviolet radiation at 210 mJ/cm^2 and developed for 60 sec in the SU-8 developer (MicroChem Corp.). The bonding strength of PDMS and SU-8 is generally poor due to the low surface energy of PDMS. This particular property is helpful for stripping off SU-8 from the PDMS surface.

The pattern formed by highly viscous photoresist was soft even after the photolithography steps due to partially cross-linked SU-8. Hence, to have more rigid pattern structures, the photoresist-coated PDMS channel was hard-baked [Fig. 1(h)] at 115 °C for 150 sec. The PDMS layer with the developed pattern was then cleaned with RF plasma in the presence of oxygen gas (Plasma Etcher PE 2000, South Bay Technology, Inc., San Clemente, California). This temporarily activated the exposed part of the PDMS and provided very good adhesion with the metal. The patterned PDMS channel was then loaded into the sputtering machine (Edwards Auto 306, BOC Edwards, Massachusetts). A titanium thin film (~30-nm thick) was deposited at 0.4 A for 195 sec followed by a platinum layer (~320-nm thick) at a dc power of 60 W for 30 min. The titanium thin film was used as an adhesion layer for platinum electrodes because the bonding strength between the PDMS and platinum is normally very weak. In microfluidic applications, usually a very high pressure is used to load sample and reagents. Therefore, a good bonding strength is necessary for integrated electrodes on the microchannel surface.

Our next step was to remove hard-baked SU-8 photoresist from the channel surfaces. The hard-baked (cured) SU-8 cannot be dissolved with any available solvents such as MicroChem's Remover PG. However, the hard-bake process aided in stripping off the photoresist from the PDMS surfaces. Moreover, it was found that the sputtering of the metals (Ti/Pt) caused increased brittleness of the photoresist. These factors helped easy peeling of the metal-coated photoresist from the PDMS surface. Using this procedure, one can avoid the use of hazardous chemicals such as aqua regia for platinum etching. The PDMS channels patterned with platinum electrodes were then cleaned with acetone, isopropyl alcohol, and DI water [Fig. 1(i)]. For permanent bonding of top and bottom layers, both layers were cleaned by oxygen RF plasma (PDC-32G, Harrick Scientific Co., New York) for 20 sec prior to the bonding. Oxygen plasma treatment renders the PDMS surface hydrophilic. This also facilitates easy loading of the sample due to the replacement of CH_3-groups with OH-groups.

3 Topography of Embedded Microelectrodes

Scanning electron microscopy (SEM; Sirion200, FEI Company, Oregon) pictures of the electrodes embedded in channels of different depths are shown in Fig. 2. These pictures were taken at different magnifications ranging from 33× to 2000×. Figure 2(a) illustrates platinum electrodes patterned on a flat PDMS surface. This was observed at 80× magnification.

In microfluidic devices, the surface roughness of electrodes is one of the most important concerns. Figure 2(b) presents the surface quality of the platinum electrode shown in Fig. 2(a). This picture was taken using SEM with 2000× magnification. Although there seem to be very tiny

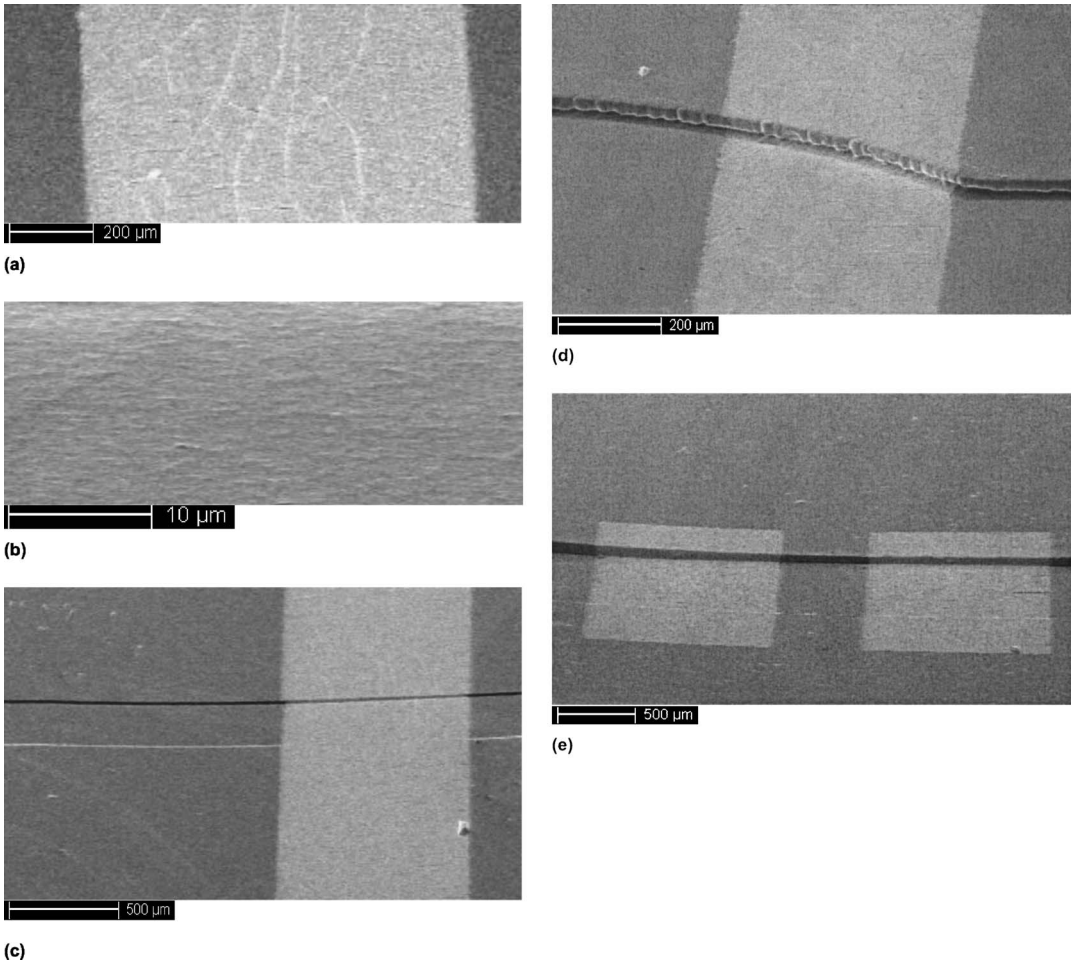

Fig. 2 SEM images of patterned platinum electrodes on a flat PDMS surface at (a) 80× magnification and (b) 2000× magnification. SEM images of patterned electrodes in PDMS microchannel for (c) 10-μm (52× magnification), (d) 50-μm (119× magnification), and (e) 200-μm (33× magnification) channel depth. Electrodes were patterned on the bottom layers in (c) and (d) and on the top layer in (e). Bottom layer electrodes were extended for wire connection with the external electrical circuit.

bumps of a few nanometers in size [in Fig. 2(b)], the overall electrode surface is highly smooth. Platinum electrodes were also successfully patterned in PDMS microchannels of different depths. Figures 2(c)–2(e) show the Pt-electrodes around 10-, 50-, and 200-microns-deep channels. These images also indicate that the side surface of the electrode is very smooth and vertical.

Figure 3(a) shows the schematic of two platinum electrodes on a PDMS surface, while Fig. 3(b) illustrates their quantitative profile. This measurement was performed by a profilometer (SPN Technology, Inc., California) which provides quantitative values with atomic resolution. From Fig. 3(b), it is clear that the surface roughness of PDMS is less than 50 nm and the surface roughness of sputtered electrodes varies between −50 nm and +50 nm. Surface roughness of PDMS mainly originates from the roughness of the microscope glass slide used in photolithography. This surface condition could be improved by using a high-quality silicon wafer during the photoresist patterning and molding processes.

The variation in platinum thickness is shown in Fig. 3(c) for different electrodes formed on different PDMS surfaces. The average thickness of platinum thin film varies between 325 and 425 nm, although the design thickness was ~350 nm. The deviation could be due to inconsistent sputtering rate over time, since the sputtering process is machine dependent. Surface roughness due to the sputtering process can be reduced by achieving high-vacuum conditions in the sputtering chamber.

4 Current Check Using Embedded Microelectrodes

This section demonstrates the sensing ability of integrated microelectrodes in a PDMS microchip. Figure 4(a) shows a photograph of a PDMS microchip with embedded platinum electrodes. For clarity, only the lower half of the PDMS microchannel is shown here. The electrodes were fabricated in the microchannel (400 microns deep) and extended outside for electrical connections. To form an integrated microfluidic system, this bottom layer was bonded with a flat PDMS (top) layer after plasma cleaning (not shown in figure). Next the microfluidic chip was tested for both liquid flow and electrical current.

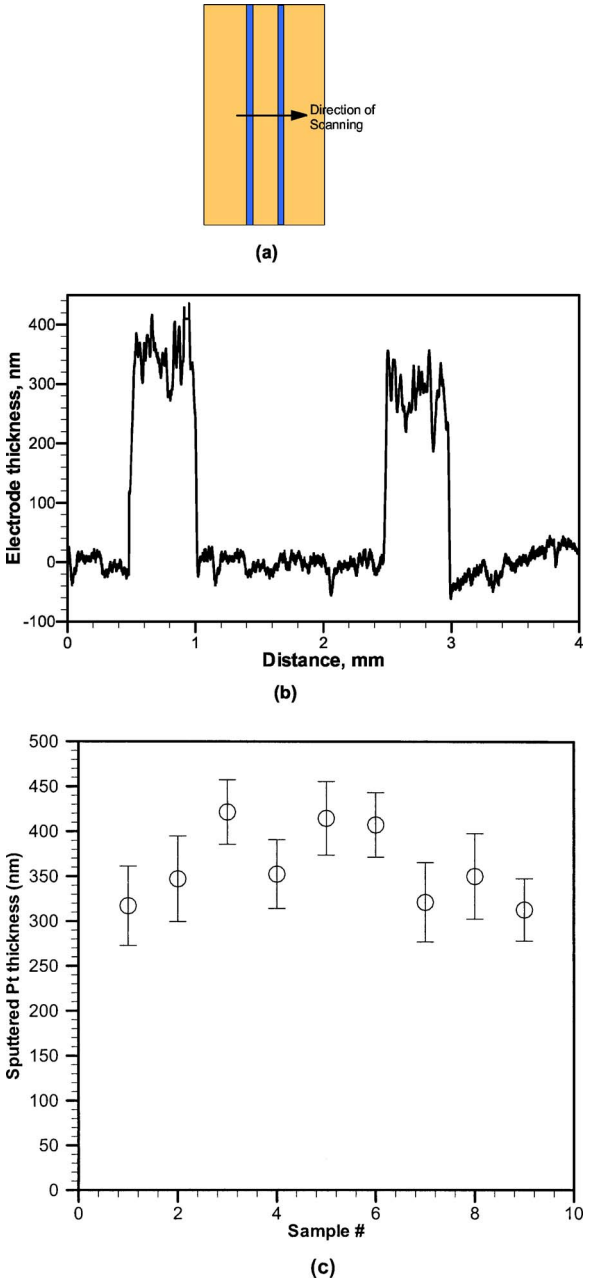

Fig. 3 (a) Schematic of the embedded Pt-electrodes on a flat PDMS surface. (b) Quantitative measurement of deposited platinum thickness on a flat PDMS surface. (c) Pt-electrode thickness measured by the profilometer for different samples. Each error bar is based on seven individual runs with a confidence interval of $\pm 2\sigma$.

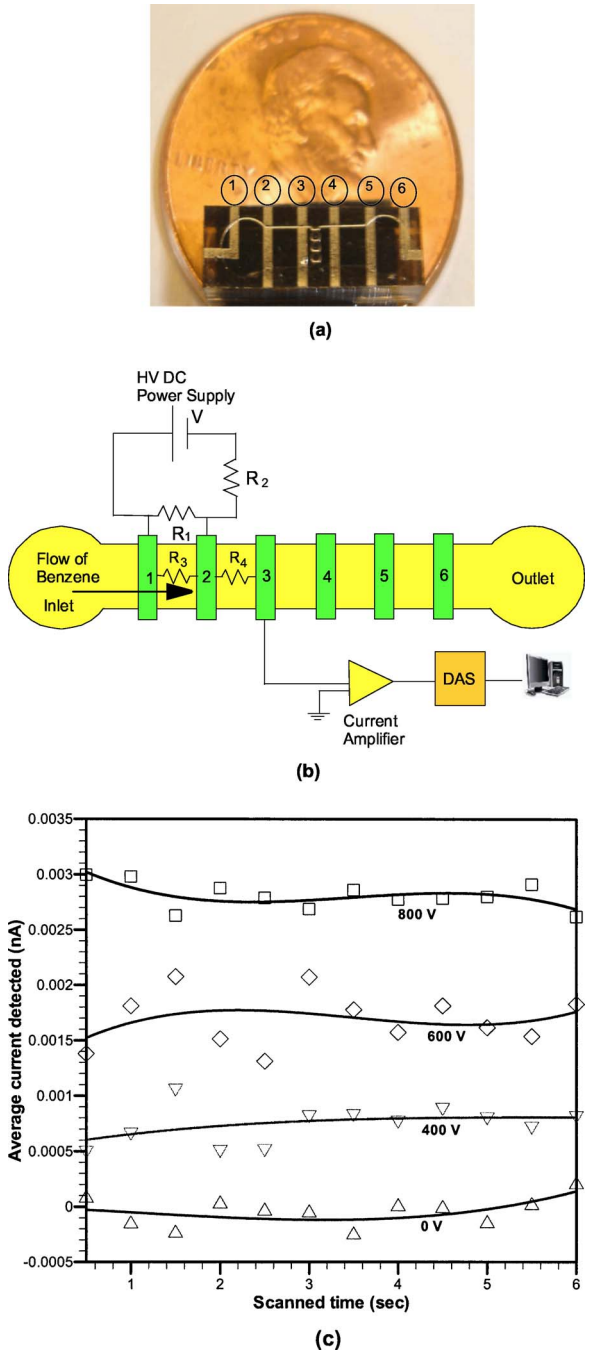

Fig. 4 (a) Photograph of the patterned platinum electrodes formed around and outside of the PDMS microchannel. (b) Schematic of the current measurement setup. Electrode #3 is used as the sensor, though electrodes #4 to #6 can also be empolyed as sensors. (c) Average current detected by the Pt-sensor (electrode #3) to demonstrate the connectivity and integrity of embedded electrodes. During current measurement experiments, a constant (benzene) flow rate of 5 μL/min was maintained through the channel.

The experimental setup, as shown in Fig. 4(b), consists of three components: fluidic circuit, electrical circuit, and detection system. In the fluidic circuit, a syringe pump was connected to the left reservoir via a capillary to maintain a constant flow rate in the microchannel. It is possible to run the flow experiment with any kind of liquid (conductive or dielectric), but in an ion mobility spectrometer, a nonpolar drift fluid such as benzene, chlorobenzene, hexane, isooctane, n-decane, or o-xylene is essential to ensure uniform electric fields between the electrodes. Thus, to demonstrate the continuity of an individual electrode, benzene was used as a buffer. The fluidic circuit was checked by passing benzene through the microchannel, and no seeping of liquid through the intersection of two layers was observed for flow rates up to 15 μL/min. Since PDMS is a highly transparent material, one can easily (visually) detect any liquid leakage through the intersection from the change of interface color.

The electrical circuit consists of a high-voltage power supply (Series 230, Bertan, Hicksville, New York), four resistors, and two electrodes (#1 and #2), as depicted in Fig. 4(b). The external resistors R_1 and R_2 were set as 1 MΩ each, while the fluid resistance (R_3 and R_4) depends on the flow geometry and buffer conductivity. The current detection system consists of electrode #3, a current amplifier (427 Current Amplifier, Keithley Instruments, Ohio), and a data acquisition system (SCB-68, National Instruments, Texas). The current detected by electrode #3 was amplified with a gain of 10^8 volt/amp. The voltage signal was then received by the data acquisition system and finally sent to a computer, where the output voltage was displayed and recorded by LabVIEW (v. 6.1, National Instruments, Texas) software. Therefore, the current measured by the sensor was obtained by dividing the output voltage with amplifier gain.

Figure 4(c) shows the current detected at different applied potentials. In this study, the current values were obtained for applied electric potentials up to 800 V. The instantaneous current values are time-averaged over an interval of 0.5 sec. When no potential was applied (V=0) from the power source, an average current of −0.048 picoA was detected by the sensor. This negligible amount of current was probably due to the electronic noise of the power supply, amplifier, and other electrical devices. Experimental results show that electric current increases with applied electric potential (V). For instance, at 400, 600, and 800 V, the average currents (through the benzene) were 0.75, 1.69, and 2.81 picoA, respectively, and the corresponding standard deviations were 1.811, 1.809, and 1.816 picoA. These smooth current responses due to the voltage change confirm the integrity and continuity of the platinum electrodes both inside and outside of the channel.

In this experiment, the measured current was very low since nonpolar benzene was used as buffer. Low current measurements (current <1 nA) often encounter noise and errors. These errors mainly originate from triboelectric effect due to the friction between electrodes and connecting wires and current leak through the PDMS materials. Triboelectric effect can be minimized by reducing the external vibration, while the leakage current can be controlled by keeping the electric field lower than the dielectric strength of PDMS.

5 Conclusions

We developed a novel platinum microelectrode fabrication technique in the PDMS-based microfluidic channel. Our electrode fabrication technique consists of lithography, thermal processing, sequential electrode sputtering, and stripping off photoresist, while soft lithography is used to form the microfluidic channels. In this study, the microchannel thickness was varied from 10 microns to 400 microns. The designed thickness of the platinum electrode was 350 nm to reduce the flow disturbances in the microfluidic chip. The surface roughness of platinum electrodes was between −50 nm and +50 nm, even for deep microchannels. The electrode patterning process presented in this study is very effective in obtaining a smooth and flat electrode surface with almost vertical sides. This microfabrication of platinum electrodes in PDMS channels offers a number of advantages. First, this process does not require use of chemicals like aqua regia. Second, it can be used for both shallow and deep microchannels. Third, no platinum residue was observed in places where platinum with photoresist was removed.

Acknowledgments

The authors thank Phillip David Hayenga for his help with SEM and Maggie Tam for LabVIEW and other electrical equipment. This work is funded by the National Science Foundation under Grant No. CTS0300802.

References

1. A. T. Woolley and R. A. Mathies, "Ultra-high-speed DNA sequencing using capillary electrophoresis chips," *Anal. Chem.* **67**(20), 3676–3680 (1995).
2. H. C. Cui, K. Horiuchi, P. Dutta, and C. F. Ivory, "Isoelectric focusing in a poly(dimethylsiloxane) microfluidic chip," *Anal. Chem.* **77**(5), 1303–1309 (2005).
3. T. Chovan and A. Guttman, "Microfabricated devices in biotechnology and biochemical processing," *Trends Biotechnol.* **20**(3), 116–122 (2002).
4. H. Becker and L. E. Locascio, "Polymer microfluidic devices," *Talanta* **56**, 267–287 (2002).
5. J. C. Mcdonald and G. M. Whitesides, "Poly(dimethylsiloxane) as a material for fabricating microfluidic devices," *Acc. Chem. Res.* **35**(7), 491–499 (2002) (and references therein).
6. T. J. Johnson, D. Ross, and L. E. Locascio, "Rapid microfluidic mixing," *Anal. Chem.* **74**, 45–51 (2002).
7. C. H. Chiou, G. B. Lee, H. T. Hsu, P. W. Chen, and P. C. Liao, "Micro devices integrated with microchannels and electrospray nozzles using PDMS casting techniques," *Sens. Actuators B* **86**, 280–286 (2002).
8. S. M. Mitrovski, L. C. C. Elliott, and R. G. Nuzzo, "Microfluidic devices for energy conversion: Planar integration and performance of a passive fully immersed H_2-O_2 fuel cell," *Langmuir* **20**, 6974–6976 (2004).
9. Y. L. Loo, R. L. Willett, K. W. Baldwin, and J. A. Rogers, "Interfacial chemistries for nanoscale transfer printing," *J. Am. Chem. Soc.* **124**, 7654–7655 (2002).
10. Y. Park, C. Chen, K. Lim, N. Park, J. H. Kim, and J. H. Hahn, "Metal thin-film micropatterns transfer on PDMS and its application to capillary electrophoresis electrochemical detection on PDMS microchip," in *Intl. Conf. on Miniaturized Chemical and Biochemical Analysis Systems*, pp. 623–626 (2003).
11. T. W. Lee, S. Jeon, J. Maria, J. Zaumseil, J. W. P. Hsu, and J. A. Rogers, "Soft-contact optical lithography using transparent elastomeric stamps: Application to nanopatterned organic light-emitting devices," *Adv. Funct. Mater.* **15**, 1435–1439 (2005).
12. M. A. Burns, B. N. Johnson, S. N. Brahmasandra, K. Handique, J. R. Webster, M. Krishnan, T. S. Sammarco, P. M. Man, D. Jones, D. Heldsinger, C. H. Mastrangelo, and D. T. Burke, "An integrated nanoliter DNA analysis device," *Science* **282**, 484–487 (1998).
13. S. N. Brahmasandra, V. M. Ugaz, D. T. Burke, C. H. Mastrangelo, and M. A. Burns, "Electrophoresis in microfabricated devices using photopolymerized poly(acrylamide) gels and electrode-defined sample injection," *Electrophoresis* **22**(2), 300–311 (2001).
14. S. M. Mitrovski, L. C. C. Elliott, and R. G. Nuzzo, "Microfluidic devices for energy conversion: Planar integration and performance of a passive, fully immersed H_2-O_2 fuel cell," *Langmuir* **20**, 6974–6976 (2004).
15. A. Hiratsuka, K. Kojima, H. Suzuki, H. Muguruma, K. Ikebukuro, and I. Karube, "Integration of microfabricated needle-type glucose sensor devices with a novel thin-film Ag/AgCl electrode and plasma-polymerized thin film: Mass production techniques," *Analyst (Cambridge, U.K.)* **126**(5), 658–663 (2001).